Tellus (2008), 60A, 427–438
Printed in Singapore. All rights reserved

TELLUS

Future wind, wave and storm surge climate in the Northern Seas: a revisit

By JENS BOLDINGH DEBERNARD[1]* and LARS PETTER RØED[1,2], [1]*Norwegian Meteorological Institute, P.O. Box 43 Blindern, N-0313 Oslo, Norway;* [2]*Department of Geosciences, University of Oslo, Norway*

(Manuscript received 2 May 2007; in final form 27 December 2007)

ABSTRACT

We consider possible changes in the future climate of wind speed (WS), significant wave height (SWH) and storm surge residual (SSR) for a region covering the Northern Seas. Our results are based on an analysis of changes in the response derived with regional atmosphere, wave, and storm surge models run for two time periods 1961–1990 and 2071–2100. Available for the study were atmospheric downscalings of the Hadley Centre's SRES A2 and B2 scenarios, the Max-Planck Institute's SRES B2 scenario and the Bjerknes Centre's SRES A1B scenario.

The most important statistically significant findings are, first, a decrease in WS south of Iceland accompanied by a decrease of about 4–6% in SWH. Secondly, there is an increase in the eastern North Sea that continues into the Skagerrak. Along the North Sea east coast and in the Skagerrak the annual 99-percentiles of SWH and SSR increase 6–8% and 8–10%, respectively, and these results are robust across the various choices in global models and emission scenarios. Finally, there is an increase in the annual 99-percentiles of all variables west of the British Isles.

1. Introduction

1.1. Motivation

We consider possible changes in the future wind, wave and storm surge climate in the northern North Atlantic, that is, the Norwegian, Greenland and Iceland Seas, together with its adjacent North and Barents Seas (hereafter referred to as the Northern Seas). The study is motivated by the concern raised in reports by the Intergovernmental Panel on Climate Change (IPCC, 2001) that there is a possibility for a rougher wave climate and increased storm surges in the Northern Seas in the future. The concern is raised based on global simulations that project possible future increases in the intensity of storms. Although different global models predict a relatively consistent rise in the global mean temperature, the regional changes are highly variable, and at the present stage, the regional effects of global climate change must be regarded as far from being conclusive. The question has become particularly relevant after the release of the Arctic Climate Impact Assessment report (ACIA, 2004) stating that the Arctic has warmed at a rate twice that of the rest of the world over the past few decades.

One important reason for these large regional differences is that the global models, and in particular, the ocean model components, are integrated forward with a grid resolution that is far too coarse to simulate the regional flow patterns in any adequate way. A remedy for this is to dynamically downscale results from an AOGCM by nesting a high-resolution regional atmospheric climate model (RACM), into a subdomain of the global model simulation, for example, Jones et al. (1995, 1997), Bjørge et al. (2000) and Haugen and Iversen (2008), or even a regional coupled atmospheric-ice-ocean model as, for instance, described by Debernard and Køltzow (2005). The results from the global model are then used as lateral boundary conditions for a regional climate simulation. Provided that the global simulation gives a realistic description of the large-scale circulation patterns, the nested high-resolution model integration may by used to project the climate variability onto the finer regional scale.

1.2. Earlier studies

One of the first studies considering a possible regional climate change in sea state and focusing on the Northern Seas was the WASA project (WASA, 1998). Their analysis was based solely on available observations of storms and waves, and concluded that the storm and wave climate in most of the Northeast Atlantic and in the North Sea has undergone significant variations on timescales of decade, and indeed has roughened in recent decades. They also concluded that the present intensity of the storm and wave climate seems to be comparable with that of the beginning of the 20th century. This is corroborated by IPCC (2001) where it is stated that based on limited data, the observed

*Corresponding author.
e-mail: jens.debernard@met.no
DOI: 10.1111/j.1600-0870.2008.00312.x

variations in the intensity and frequency of tropical and extratropical cyclones and severe local storms show no clear trends in the last half of the 20th century, although multidecadal fluctuations are sometimes apparent. However, Pfizenmayer and von Storch (2001) found an increase in the frequency of eastward propagating waves in the central North Sea that significantly deviates from what is expected given their analysis of natural variability. By comparing with results from downscaled AOGCM scenarios they suggest this change is a local manifestation of anthropogenic global climate change. Regarding storm surges Langenberg et al. (1999) analysed changes in mean and extreme sea level due to storms around the North Sea with statistical and dynamic methods. For the extreme events they concluded that the natural variability is too large to detect any significant changes.

In a series of studies utilizing empirical downscaling methods relating seasonal mean sea level pressure from AOGCMs to wave height, Wang et al. (2004), Wang and Swail (2006) and Cairesa et al. (2006) find large variations in the predicted changes in the Northern Seas due to differences in emission scenarios and to the choice of global models.

In an earlier study, Debernard et al. (2002) (hereafter DSR) make projections of the future regional wind, wave and storm surge climate in the Northern Seas based on an atmospheric downscaling of one of the earlier IPCC scenarios [the Max-Planck Institute's (MPI) global GSDIO scenario]. Their method was to first make a dynamic downscale of the global climate scenario using a regional atmosphere model, and then use these downscaled wind and sea surface pressure scenarios as forcing for stand alone wave and storm surge models. They found that the changes in the Northern Seas wind, wave and storm surge climate, with a few exceptions, were mostly small and insignificant. However, other studies using regional storm surge models (Lowe et al., 2001; Lowe and Gregory, 2005; Woth, 2005; Woth et al., 2006) have found statistically significant increases in extreme surge events due to greenhouse gas forcing in the North Sea. Note that we also include the two Hadley Centre (HC) global scenarios used by Lowe and Gregory (2005) and Woth (2005) in this study, except that we use a different RACM and a different computational domain when downscaling the regional atmospheric response.

1.3. This study

In view of the findings reported in the recent Arctic Climate Impact Assessment report (ACIA, 2004), we think it would be useful to investigate whether the results reported by DSR and Lowe and Gregory (2005) carry over when dynamically downscaling more recent IPCC scenarios, in particular those used by ACIA (2004). Since we use the same method and computational domain as DSR, this study is a straightforward extension of their work to include new climate change scenarios.

The new scenarios used here are the global SRES A2 and B2 simulations from the HC's atmospheric global climate model (AGCM) HADAM3H (hereafter referred to as HADA2 and HADB2, respectively), one SRES B2 simulation from the MPI's AGCM ECHAM4 (hereafter referred to as MPIB2), and one SRES A1B simulation from the Bjerknes Centre for Climate Research's (BCCR) global coupled climate model BCM (hereafter referred to as BCA1B). The A2 scenario has a rapid increase in the emission of greenhouse gases while the B2 scenario is among the more moderate scenarios used in the IPCC TAR (IPCC, 2001). The A1B is intermediate between the others but closest to the B2 scenario. For comparison the earlier GSDIO-simulation from MPI used by DSR is based on the IS92a scenario with a slightly higher increase in the emissions than the B2 scenario.

As in DSR we base our calculations on dynamic downscaling of these global scenarios. A detailed description of the downscaling procedure and of the atmospheric results is found in Haugen and Iversen (2008). The RACM they used is the HIRHAM model (Christensen et al., 1997; Christensen and Christensen, 1998; Bjørge et al., 2000). The downscaled results consist of two time-slice periods of 30-yr each, one from 1961 to 1990 and a second from 2071 to 2100. We refer to these periods henceforth as the control and the future climate, respectively. The difference between the two time-slices thus yields one possible regionalized climate change scenario over a 110 yr period.

We start by describing the wave and storm surge models used (Section 2). This is followed by a description of the analysis method we apply (Section 3), and a discussion of the results (Section 4). Finally, we offer a brief summary and some conclusions in Section 5.

2. Models

As in DSR we derive the projected wave and storm surge climate by using state of the art wave and storm surge models. The models we use are those employed operationally by the Norwegian Meteorological Institute to provide daily forecasts of waves and storm surges for Norwegian waters (e.g. http://met.no/kyst_og_hav/havvarsel.html). The wave model (MIWAM) is a locally implemented version of the WAM model (WAMDI-group WAMDI, 1988) with upgrades in accord with the changes reported by Bidlot et al. (1997). The storm surge model (MIPOM) is derived from the widely used Princeton Ocean Model (POM) (Blumberg and Mellor, 1987) as documented in Engedahl (1995) and Engedahl et al. (2001). While the wave model was integrated on a computational domain and grid equal to the one employed in the RACM downscaling, the storm surge model was implemented on a separate grid as detailed in DSR. These domains are shown in Fig. 1 together with the location of the stations used for the storm surge analysis (Section 4.4). To exclude the direct effect of the open boundary conditions, and to reduce the amount of stored data, a smaller domain (shown in Fig. 4) is used for the storm surge analysis. As atmospheric forcing we utilized the 10 m winds from the atmosphere model every sixth hour, and for

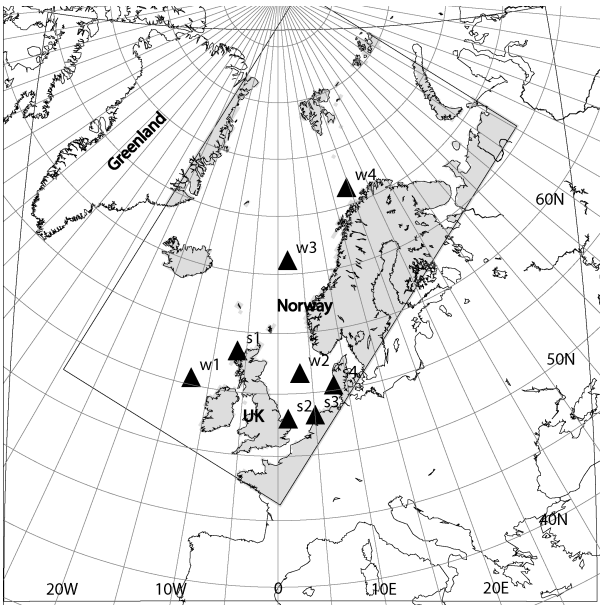

Fig. 1. Geographical area covered by the regional atmosphere model used in the downscaling and the wave model. Also shown is the domain used by the storm surge model (inner frame) in addition to coastal stations and offshore positions used for analysis of the change in the largest storms in Section 4.4. The coastal stations are s1: Stornoway, s2: Lowestoft, s3:Texel Noordzee, and s4: Esbjerg, while the offshore stations are w1: Buoy K4 near Rockall, w2: Ekofisk, w3: Weather ship MIKE and s4: Tromsøflaket.

the storm surge model we also used the mean sea level pressure every sixth hour. For more details on the model setups we refer to DSR.

Note that also tidal forcing is included in the storm surge runs to account for the sometimes important non-linear interaction between tides and water level changes due to atmospheric forcing. However, since we do not wish to keep the tidal contribution in the analysis we adopted the following procedure to detide the results. First we made a simulation including both tidal and atmospheric forcing. Then we made a simulation with tidal forcing only, and simply subtracted the latter from the former. With this approach we are left with water level variations due to variability in atmospheric winds and pressure together with possible non-linear tide-surge interaction effects, while omitting the dominating tidal signal. Finally, we note that due to the mostly additive nature of mean sea level on storm surges (Kauker and Langenberg, 2000; Lowe et al., 2001), we have not included possible changes in mean sea level due to other effects in the simulations.

3. Analysis method

3.1. Time-series

The production by use of the above model systems results in seven 30-yr-long time-series at the respective model grid points for each of the variables, namely wind speed (WS), significant wave height (SWH), and what we here refer to as storm surge residual (SSR). The latter is defined as the water level minus the astronomical tide. Of these seven series, three represents the downscaling of the various global models rendition of today's climate (control), while the remaining four are simulations of the future climate.

We analyse the time-series by comparing different statistical measures (see Section 3.2) from the control with the same statistics from the scenario. The statistics are defined over a year or a season. Thus, from one control period we get 30 values of the statistics which constitutes a population with a spread defined by the interannual variability. We then compare this population with the population from its respective scenario to check if there is a significant difference between the two. Because the populations are generally not normal distributed, we apply the Wilcoxon rank-sum test rather than the more common Student's *t*-test (Bhattacharyya and Johnson, 1977). However, alternative tests with the Student's *t*-test show that the results are robust with respect to the choice of method. A probability less than 5% thus means that the chance that the two 30-yr time-series comes from the same population is less than 5%. If this is the case we consider the difference to be statistical significant on the 95% confidence level. In the figures presented in Section 4 we have shaded the areas were this level is less than 95% in light grey (e.g. Fig. 2).

In addition to comparing the changes for each individual scenario, we also define a multimodel population by collecting the same statistical measures from different simulations into one population for the control and one for the scenario before the statistical tests are evaluated. To avoid a bias in the populations towards the climate and response of the HC model, the combined analysis utilizes only the HADB2, MPIB2 and BCA1B scenarios. We prefer the HADB2 scenario over the HADA2 since this gives us a more homogeneous group of emission scenarios.

We present the results from these statistical analyses by showing fields of the *relative* change in the population mean between the scenario and control periods. The relative change in a quantity V is defined as

$$C_V = \frac{V_{Sc} - V_{Ctr}}{V_{Ctr}} \times 100, \quad (1)$$

where C_V denotes the change experienced in V, while the subscripts Sc and Ctr denote, respectively, the future climate value (scenario) and control value of V.

3.2. Statistical measures

As changes in the extreme statistics are the most important for society we mainly focus our analysis on the extremes. Nevertheless, we have also analysed changes in the mean climate as well. In this respect, note that although the mean WS and mean SWH are considered robust measures of the overall wind and

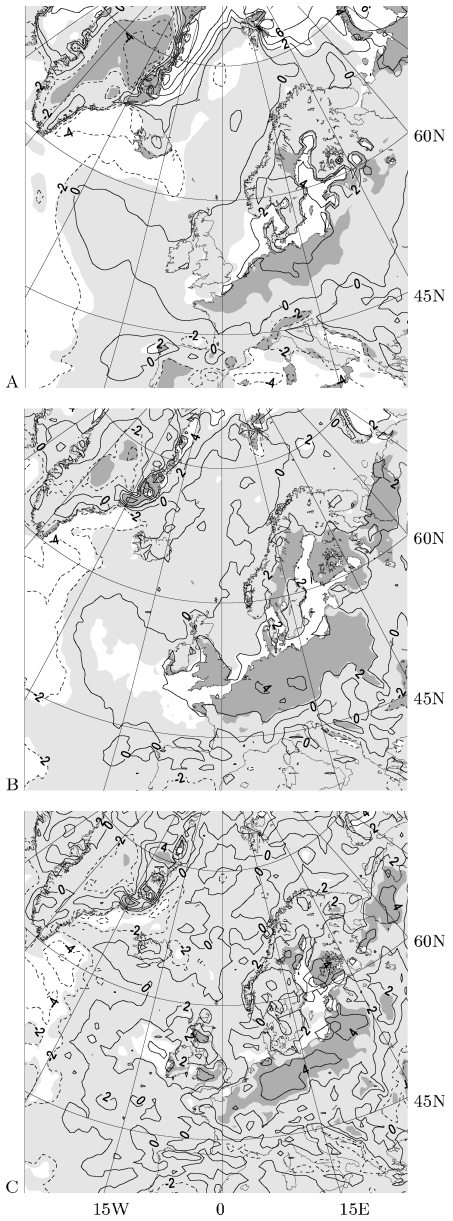

Fig. 2. Relative changes (in percent) in wind from the combined analysis of the HADB2, MPIB2 and BCA1B scenarios. (A) Annual mean, (B) Annual 99-percentile, (C) Annual maximum. Solid lines are positive values, dashed lines indicate negative values. The light grey-shaded region indicates areas where the changes are insignificant from the statistical test, while white and dark grey shaded areas denotes areas where the changes are statistically significant over ocean and land areas, respectively.

wave climate, respectively, this is not the case for the SSR. As the mean SSR is always close to zero, we regard the standard deviation of SSR to be a more appropriate robust measure of the 'mean' surge climate.

As relatively robust measures of the extreme events we use the annual and seasonal 99-percentiles. In addition, annual maximum values are used to represent the most extreme cases. These quantities are based on all of the data in the time-series, that is, 6-hourly values for WS and SWH and 1-hourly values for the SSR.

To investigate the extreme events more closely, we have also extracted the 100 highest events of SWH and SSR from each time-slice at selected locations. In each series, the events are sorted in ascending order. To prevent one storm from biasing the extremes the events are selected such that there is a time span of at least 48 h between any two events. In this way, we assume that each event represents an individual, independent storm. A qq-plot of the events from the scenario against the events from the control, is then indicative of a change in the wave or storm surge climate if there is a significant deviation from the 1:1 line.

As a complement to the qq-plot we have furthermore made a closer analysis of the relative change of the 10 largest events from the scenario and control. Sorted in ascending order, the events in both the control and scenario are given ranks from 1 for the highest event and up to 10 for the 10th highest event. Then, by using eq. (1), the relative difference is defined by comparing the events with the same rank from control and scenario. We present the results as functions of the rank number.

4. Analysis and discussions

4.1. Annual statistics

We start by showing results from the combined multimodel analysis. As revealed by Fig. 2, the horizontal patterns of the *relative* differences in annual mean, annual 99-percentile and annual maximum of WS are very similar. Generally, they show a reduction in WS near the western boundary of the domain, and an increase (2–4%) from west of the British Isles and eastward over the North Sea, European continent north of the Alps, and also northward into the Baltic Sea. This is a robust feature in the results and, as discussed shortly, it is accompanied by significant changes in the wave and surge climates (Figs. 3 and 4, respectively). The increase in the eastern part of the domain is consistent with an decreased return period of high wind events, as found by Haugen and Iversen (2008) when analysing the same wind data.

We also observe statistically significant increases of 2–8% in annual mean WS over the area normally covered by sea ice in the Fram Strait and Barents Sea. However, the changes are less pronounced in the annual 99-percentile and maximum. These changes over the areas where the control has sea ice that is not present in the scenario are considered uncertain. The reason is in part due to the special handling of sea ice necessary in the downscaling procedure (Haugen and Iversen, 2008), and in part because of the uncertainties in the sea ice distribution from the underlying global model runs.

The changes in annual mean, annual 99-percentile and annual maximum of WS south west of the British Isles merits some

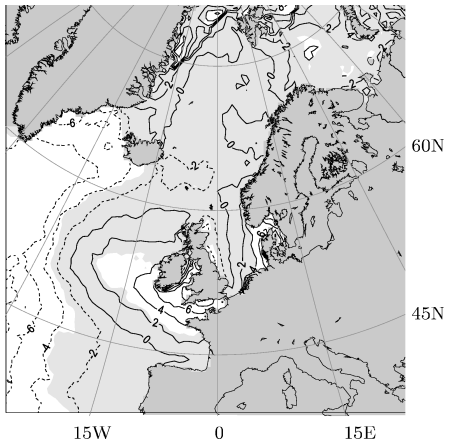

Fig. 3. Same as Fig. 2, but displaying relative changes in annual 99-percentile of SWH from the combined analysis of the HADB2, MPIB2 and BCA1B scenarios.

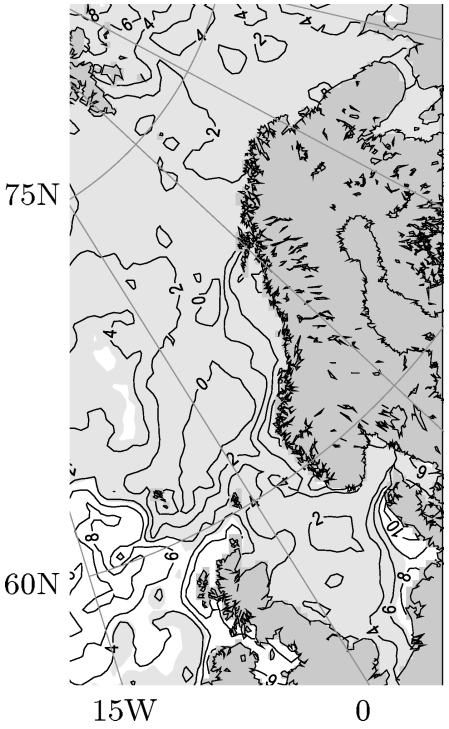

Fig. 4. Same as Fig. 2, but displaying relative changes in annual 99-percentile of SSR from the combined analysis of the HADB2, MPIB2 and BCA1B scenarios. The domain is truncated compared to the whole computational area depicted in Fig. 1 to exclude the direct effect of the open boundary FRS zones. In addition, most areas normally covered with sea ice, are omitted to reduce the amount of data stored for the analysis.

remarks. We observe that although the changes are significant in the 99-percentile this is not the case for the mean and maximum of WS. The main contributions to the increase in WS in this particular region are changes in the winter season. Because the strongest winds are observed during this season they also give a larger change in the 99-percentile and maximum than in the annual mean. In addition, there is a larger interannual variability in annual maximum WS than in annual 99-percentile. Consequently, the analysis only reveals the changes in the 99-percentile as being statistically significant.

Since there in theory is a strong relationship between wave height and wind, we expect changes in WS to be reflected in the SWH fields. In fact, for fully developed wind waves, not limited by fetch effects, we have $\mathrm{SWH} = 0.0246 \times (\mathrm{WS})^2\ \mathrm{s}^2\ \mathrm{m}^{-1}$ (WMO, 1998), which for small changes in WS gives a relative change

$$C_{\mathrm{SWH}} \approx 2\, C_{\mathrm{WS}}. \tag{2}$$

Thus, we expect the change in SWH to be larger than for WS. Indeed, comparing Figs. 2B and 3 we observe that the distribution of annual 99-percentile of SWH is closely connected to that of the annual 99-percentile of WS. Examples are the significant decrease in SWH observed in the Atlantic Ocean west of 30°W (of approximately −6%) and the significant increase west of the British Isles of up to +6%. Additional important examples are the significant increase in the eastern North Sea and in the Skagerrak (6–8%).

Somewhat surprisingly we observe that the area of statistically significance in SWH is actually expanded compared to that for WS. We should keep in mind though that SWH depends not only on WS, but also on the wind fetch and the frequency and periods by which the wind changes its directions. For instance a change in the wind direction may cause a change in the SWH, in particular in coastal areas and seasonally ice covered areas, without any change in the WS. For example we see this along the east cost of United Kingdom (UK) where the SWH is decreasing while there is a small increase in WS. This response is due to a more westerly wind-field (not shown), which causes the SWH close to the coast to be fetch limited. The same sort of reduction is also found in the annual mean SWH (significant change of −2 to −4%) at this location (not shown). Accordingly we interpret the observed differences in relative change and the size of the area of statistically significance between WS and SWH as indicating changes in other conditions as well.

As evident from Fig. 4, the annual 99-percentile of SSR, shows some of the same response as the SWH, but with local differences. In this regard we note that the dependency of the storm surge response on wind is even more compound than for waves. The response not only depends on the WS and wind direction, but also depends on the movement of the storm centre as for instance shown by Gjevik and Røed (1976) and Martinsen et al. (1979). In addition, a storm surge usually propagates along the coast as a trapped planetary wave. Therefore, a single storm surge event has the potential of affecting a large area, but its local impact depends on the local coastline geometry and topography as well. Accordingly, how a specific location is affected by a storm surge is highly dependent on the movement of the storm that generates it and on the local topology. Even small changes in wind direction are crucial to whether a specific site experiences

a high surge or not. We should also keep in mind that large storm surges are mainly experienced in shallow waters or at sites close to the shore. Inherently, the impact of storm surges therefore has a very local character and is highly influenced by local coastline geometry and bottom topography.

With this in mind and with reference to Fig. 4 we note that in areas along the coast of the Netherlands, in the German Bay, and along the west coast of Denmark, there are significant increases in the 99-percentile of SSR (6–10%). In the Skagerrak and Kattegat the increase in SSR is 4–6%, but only spotwise significant along the Swedish coast (not visible from the figure). This contrasts the significant increase in SWH of 6–8% (Fig. 3) and in WS of 3% (Fig. 2B) found in this area. There is also a significant increase in SSR of the order of 6% at the northwest coast of British Isles that coincides with the increases in WS and SWH.

4.2. Seasonal statistics

We now turn to the change in seasonal mean SWH during winter (DJF) and summer (JJA) from the combined analysis (Figs. 5A and B, respectively). The winter picture shows much of the same change as found in the annual 99-percentile of SWH in Fig. 3, indicating that the winter season has the strongest storms and highest SWH also in the future. The annual 99-percentile is therefore dominated by the winter situation. These strong storms also appears to have a clear influence on the seasonal mean winter climate in general. The increase observed in the annual 99-percentile of SWH just west of the British Isles is replaced by a significant decrease during the summer season (Fig. 5B), which in turn is accompanied by an increase in WS and wave heights off the Iberian Peninsula. The change in this latter location is consistent between all scenarios.

We also note with interest that the increase in SWH found along the east coast of the North Sea in the annual 99-percentile is also found during the winter and summer seasons. Together with the decrease near the western boundary of the model domain, we find this to be the most consistent change in all of the simulations.

Because the high storm surge events are of great importance for society, and the fact that the yearly extreme statistics are dominated by winter conditions, we only present storm surge results for this season. Most of the winter 99-percentiles from the individual scenarios in Fig. 7 show similar relative changes as found in the annual 99-percentile from the combined analysis in Fig. 4.

4.3. Differences between individual scenarios

We now turn our attention to the four individual scenarios and differences between them. As revealed by Fig. 6 the largest changes from the control in annual 99-percentiles of SWH are experienced in BCA1B followed by HADA2 and HADB2. In contrast the changes in MPIB2 are mostly small and the areas of statistically insignificant changes larger. Another striking feature of interest is the *similarity* between the two very different emission scenarios of HADA2 and HADB2 and the *dissimilarity* between the two equal emission scenarios of HADB2 and MPIB2. Nevertheless, all the scenarios show a decrease in SWH in the western part of North Atlantic, an increase in the eastern North Sea, and an increase in the Skagerrak. The increase west of the British Isles found in the 99-percentile of SWH in the combined analysis (Fig. 3) is found in all scenarios except MPIB2, but is only evident in BCA1B for the annual mean SWH (not shown). This supports the conclusion that the increase in annual 99-percentile of SWH west of British Isles (Fig. 3) is mainly due to changes in the winter storms.

Several of the same characteristic responses are seen in the winter 99-percentile of SSR in Fig. 7 when comparing the individual model scenarios. Again, we note the similarity in the changes between HADA2 and HADB2, and the dissimilarity of the MPIB2 with the other three. The increases in 99-percentile of SSR around the German Bay, and at the west coast of the British Isles are found in HADA2, HADB2 and BCA1B

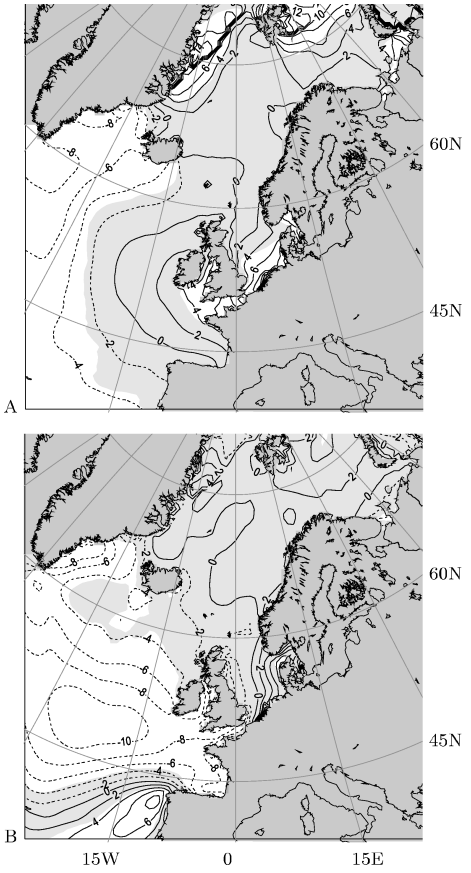

Fig. 5. Same as Fig. 2, but displaying relative changes in seasonal mean SWH from combined analysis the combined analysis. (A) winter (DJF), (B) summer (JJA).

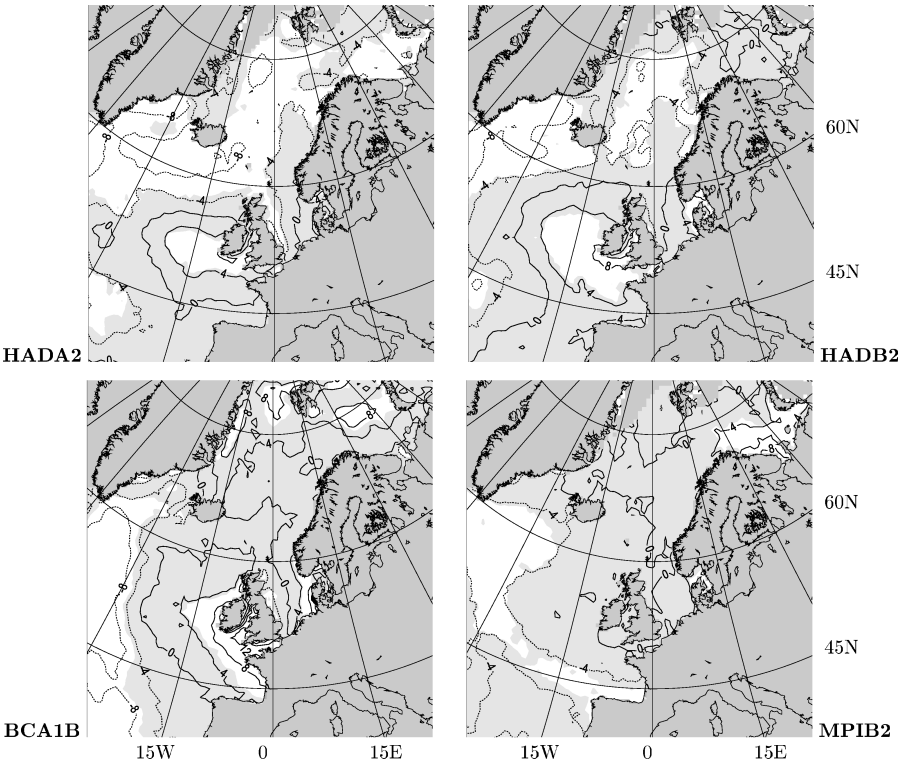

Fig. 6. Same as Fig. 2, but displaying relative changes in 99 percentile of SWH from the HADA2, HADB2, BCA1B and MPIB2 scenarios.

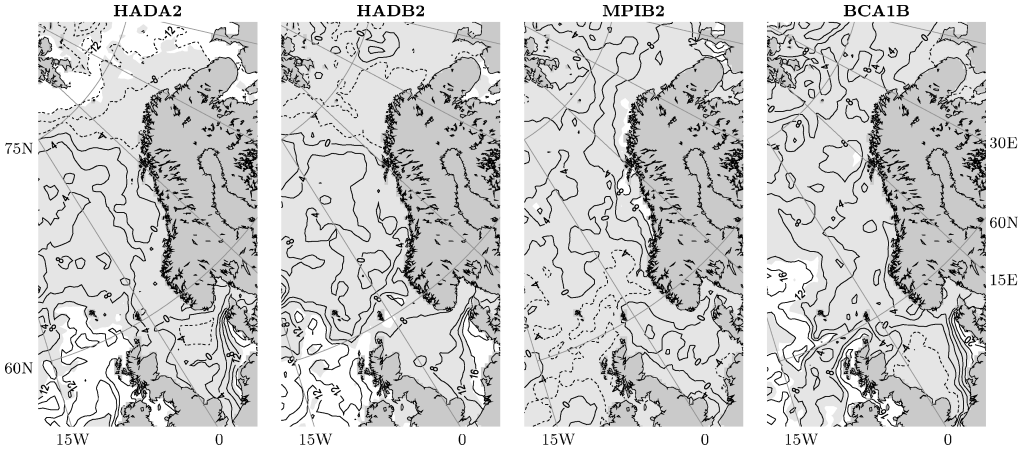

Fig. 7. Same as Fig. 2, but displaying relative changes in 99-percentile of SSR for the winter season from the HADA2, HADB2, MPIB2 and BCA1B. The depicted domain is truncated as in Fig. 4.

scenarios, while the MPIB2 shows small insignificant decreases in these areas.

As the emissions of greenhouse gases in the A2 scenario are quite larger than the emissions of the B2 scenario, it is common to expect that the changes in the future climate of WS, SWH and SSR in general are larger in the A2 scenario compared to the B2 scenario. Somewhat to our surprise we note that in general the changes in the SWH in HADB2 are actually larger than those in HADA2 (Fig. 6). As evident from the same figure this is also true for the SSR response in the south eastern part of the North Sea. These results contrasts those reported in the recent studies by Wang et al. (2004) regarding waves and Woth (2005) regarding storm surges. We note, however, that the results for the A2 scenario in Wang et al. (2004) shows both increases and decreases in SWH, and the regional consistency of the changes between the different scenarios are generally low (Wang et al., 2004; Wang and Swail, 2006; Cairesa et al., 2006). We also note that in the wind scenarios shown by (Räisänen et al., 2004, their figs 7 and 10), and which were used by Woth (2005), it is evident that in large areas their downscaled winds from the HC

A2 scenario actually show weaker winds than their downscaled HC B2 winds. The latter supports our findings, but it should be mentioned that in their maximum winds, they do get an increase in A2 compared to B2 over the southern North Sea that explain the results reported by Woth (2005). We do not find any such enhanced increase in HADA2 compared to HADB2 in our maximum winds in this area, thus indicating a clear difference in the response of the two RACMs. Contrary to the results for the HC scenarios, the MPI scenarios reported by Räisänen et al. (2004) show a larger increase in WS for A2 than for B2. Their change in the MPI B2 scenario is also larger than we get for our MPIB2 simulation. These differences are most likely due to the differences in the physics of the RACMs and differences in the computational domains.

4.4. Changes in extreme events at selected locations

As an important issue to address is what happens to the extreme high wave and high surge events in a warmer climate, we find it worthwhile to have a closer look at the extremes via a storm analysis. To this end Figs. 8 and 9 show results related to the change in isolated extreme events for wave and storm surge, respectively, at the stations shown in Fig. 1. The left-hand columns of these figures show a so called qq-plot where the 100 severest events in each scenario is plotted against the 100 largest events from the control period. The right-hand column show the relative difference (in % as defined by eq. 1) between scenario and control for the 10-largest events from each scenario and ordered after the rank of the events. Event rank 1 is the results from the highest event in both control and scenario, while rank 10 is from the 10th largest event in both periods. In addition, the mean and standard deviation of all 40 (10 events $\times$ 4 scenarios) estimates of the relative change is given in the relative difference figures. To compare with the results from the combined analysis, the numbers in the parentheses are the mean and standard deviation based on the 30 events from the HADB2, MPIB2 and BCA1B scenarios only.

We note from the qq-plots that both SWH and SSR show large differences between the individual scenarios. Apparently, the MPI scenario is much more energetic than the others giving higher waves and surge events, while those based on the BCCR simulations are the least energetic. This might in part be a consequence of the differences in the global model scenario used for the downscaling. Differences in global model resolution and physics give boundary conditions for the regional atmosphere model that influence the interior storm climate in the regional model. The relative difference plot is a convenient way of comparing the actual change in extreme events between the scenarios despite the large differences in model climates.

Generally, we note that the results from these analyses confirm the results for the annual 99-percentiles in Figs. 3 and 4 quite nicely. Examining the relative difference for SWH we find a tendency for the largest events to be higher in the future climate. The figures for the mean relative difference indicate an increase in the highest events of 3–4%, but we observe that the standard deviation for most sites is as large as or larger than the mean difference. We also observe that the two HC scenarios have a tendency to give the same sign of the response at a selected site for a selected rank. Due to their common control period they use the same event to represent the control climate, and therefore, the calculated relative differences are not independent between the two scenarios. This gives a bias in the pictures towards the response of the HC model. However, excluding the HADA2 scenario, the figures in parentheses still show a small increase in the largest 10 events.

The same comments as for the SWH are valid for the extreme SSR events. We find, however, a larger spread in the relative changes of the high SSR events than for the high SWH events. This is also reflected in a higher standard deviation in the relative differences. For instance Lowestoft situated at the west coast of the North Sea shows no relative change in the mean, but a high variability among the estimates. The results from BCA1B shows a considerable relative change in the highest events at Stornoway located in the northwest corner of Scotland, but this is not found in the other scenarios besides the change in annual and winter 99-percentiles in Figs. 4 and 7. On the other hand, the increase we find in the in extreme SSR at Esbjerg in the 99-percentile plots is also evident when the individual events are investigated. This is the only site where the mean relative change in the 10 largest events is considerable greater than the standard deviation among the estimates. Despite the short distance between the stations Texel Nordzee and Esbjerg, there are large differences in the change. This underlines the findings of Debernard et al. (2002), stressed in Section 4.1, that the storm surge experienced at a specific location depends on the movement of the storm, the wind direction and local conditions in coastline geometry and topography.

5. Conclusions and some final remarks

We present a study that is an extension of that of Debernard et al. (2002). It covers the same area, employs the same method of regional downscaling of global scenario simulations, and uses the same wave and storm surge models. The difference is in the scenarios, the length of the time-slices, the periods chosen as control and future climate, and the combined analysis of results from all the scenarios.

Simulations of four emission scenarios are studied, namely the Max-Planck Institute's SRES B2 scenario simulation (MPIB2), the HC's SRES A2 and SRES B2 scenario simulations (HADA2 and HADB2, respectively), and the Bjerknes Centre's SRES A1B scenario simulation (BCA1B). We therefore analyse results from a total of seven 30-yr time-series of WS, SWH and SSR. From these 30-yr time-series we extract annual and seasonal statistical measures (mean for WS and SWH, standard deviation for SSR, maximum and 99-percentile for all variables). The

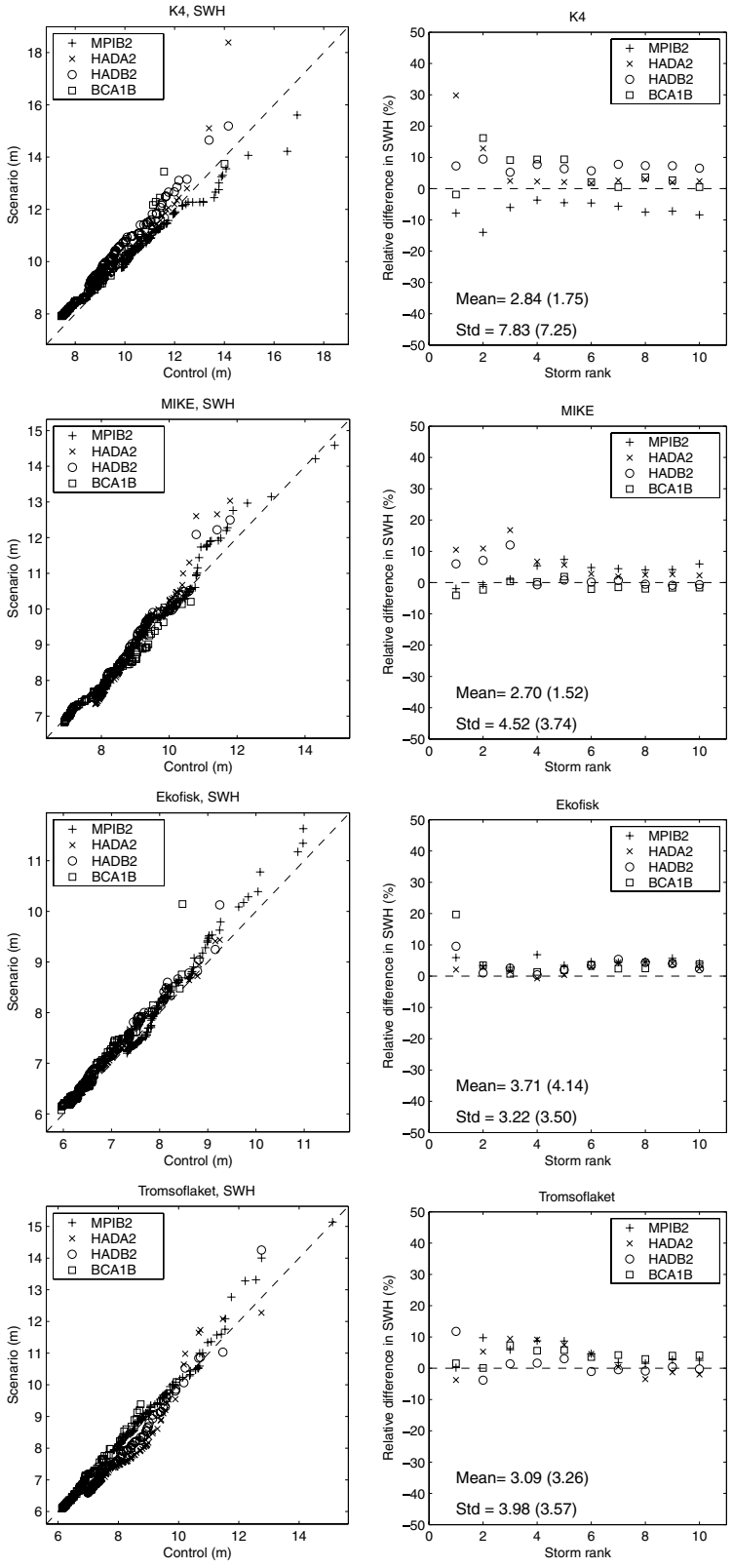

Fig. 8. Left-hand column shows qq-plots of SWH for the 100 largest events from the scenario plotted against the 100 largest events from the control period. Right-hand column shows the relative difference in percent of SWH (from eq. 1) for the 10 largest events, numbered after event rank such that the leftmost point show the relative difference between the largest event in the scenario, versus the largest event in the control. The numbers gives the mean and standard deviation (*SD*) of all the data points in the figure. The numbers in parentheses gives the same numbers excluding data points from the HADA2 scenario.

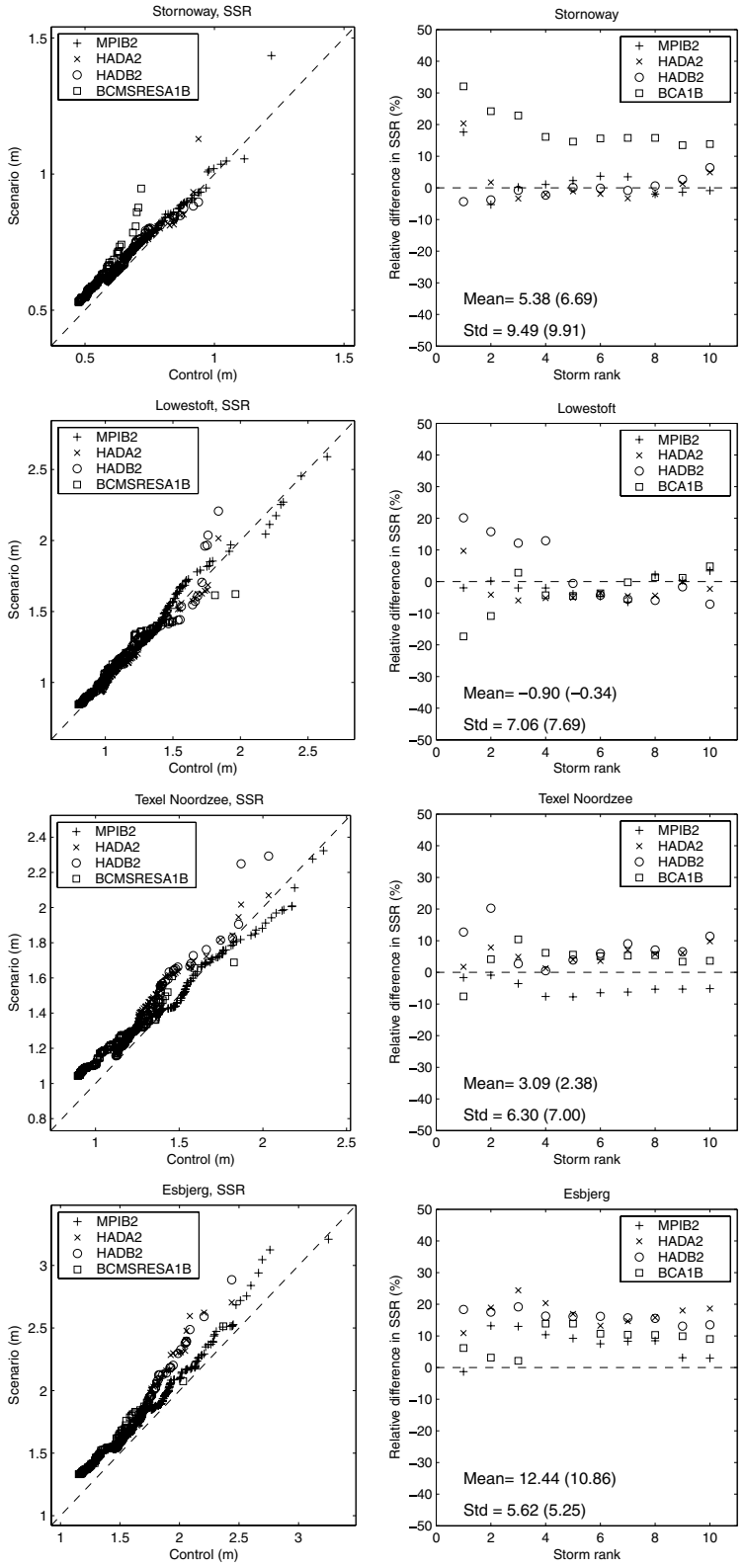

Fig. 9. Same as Fig. 8, but showing the results for the storm surge residual.

difference between the control and the future climate is analysed by comparative analyses.

The most robust result we find is a decrease in WS and SWH in the open ocean areas southwest of Iceland. This decrease is statistically significant and is approximately 6% for the annual 99-percentile of SWH from the combined analysis. The decrease is most pronounced in HADA2 and HADB2, but it is significant in all simulations.

Another important, robust result that we find is that there are considerable increases in the SWH and SSR along the North Sea east coast and in the Skagerrak. The changes in the annual 99-percentile of SWH and SSR are 6–8% and 8–10%, respectively, from the combined analysis. For SWH, the changes are evident in all simulations and for all seasons, and constitute the most robust signal in these simulations. In addition, this roughening of the SSR climate is in accordance with the results from STOWASUS-2001 (2001), Lowe et al. (2001), Lowe and Gregory (2005), Woth (2005) and Woth et al. (2006). It is, however, somewhat contrary to the results from Debernard et al. (2002) who found a minor, insignificant change in this area only. Interestingly, the ECHAM4 global model used in Debernard et al. (2002) is the same as used in the MPIB2 scenario, but with a different emission scenario. The changes in SSR in the North Sea from the MPIB2 scenario is smaller and less significant than from the other models.

Also, the annual 99-percentiles of SWH and SSR, in addition to the winter mean for SWH, show a significant increase just west of the British Isles. This increase is evident in BCA1B, HADA2 and HADB2, but not in MPIB2. It is most likely linked to a change in the winter storm track in the first three and the change is not significant in the annual mean statistics.

Based on the analysis we also note that, as expected, the changes in the future wave and storm surge climate are in accord with the change in the wind climate. The largest changes are detected in BCA1B, but there is a substantial dissimilarity between the two B2 scenarios (HADB2 and MPIB2, respectively). In contrast, there is a strong similarity between the two scenarios based on input from the HC's global scenario simulations (HADB2 and HADA2). Therefore, the uncertainty associated with projecting the future wind, wave, and storm surge climate appears to be more linked to which global climate model system is used, rather than which emission scenario is selected.

We find that there is a considerable difference between the climates of the simulations from different centres. The MPIB2 control wind climate appears to be much more energetic than the others, giving higher wave and surge events, while the BCCR control is the least energetic. Of the three global models, the BCCR model has the coarsest resolution on the boundary fields for the atmospheric downscaling (T42), while the resolution in the data from the HC and MPI is better (near T106). This leads us to ask how good are the controls really? Although this question is pertinent we have not made any attempts to perform such a validation. The underlying assumption is that the relative change gives a representative measure of the change due to a warmer climate.

We emphasise that the results near the ice edge are severely hampered by the treatment of sea ice in the global scenarios. This has a decisive influence on the atmospheric downscaling. As is well known, the different global models give very different seasonal ice covers. Hence downscaling of scenarios from them are expected to produce large discrepancies in the downscaled WS climate in these areas, which in turn impacts the projections of future wave and storm surge climates. One way to avoid this problem is to replace the atmosphere alone model by a fully coupled atmosphere-ice-ocean model to let the ocean and sea ice be a coupled and interactive part of the downscale. With a regional coupled atmosphere-ice-ocean model, as for instance described in Debernard and Køltzow (2005), the model is able to produce its own ice cover, consistent with, and in response to the local atmosphere-ocean interactions.

The analysis of relative difference for the 10 largest storms from each time-slice period indicates a small, but consistent increase in SWH (3–4%) and SSR (-1 to 12%) at selected coastal and offshore locations. This finding is consistent with the analysis of Haugen and Iversen (2008) showing a reduced return period for the present-day extreme WSs, which indicates stronger or more frequent strong storms. In addition, it is consistent with analysis of changes in daily maximum wind in the North Sea made by Beniston et al. (2007) regarding other downscalings of the HC A2 scenario. We note that this is also consistent with the results of Lowe and Gregory (2005) showing increased 50-yr return values for storm surges around the British Isles and in the North Sea, and Woth (2005) and Beniston et al. (2007) showing increased storm surges in the southeastern North Sea. Also global empirical downscaling methods show changes in the return frequency of extreme SWH events in the Northern Seas (Wang et al., 2004; Wang and Swail, 2006; Cairesa et al., 2006). However, the uncertainties due to the choices of emission scenarios and global models are considerable.

Finally, based on the possibility of more frequent strong wind events, society should prepare for higher extreme surge and wave events in the future. However, it is difficult to give uncertainty estimates for the changes, and this is especially true if we concentrate on specific locations. As shown in this study, large differences in the estimated future change are found over small horizontal distances even within the North Sea.

6. Acknowledgments

The authors thank Jan Erik Haugen for making the downscaled results available to us, and to Jon Albretsen for running the WAM wave model. This research was supported in part by the Research Council of Norway through the national climate project RegClim (Grant No. 120656/720). Support for computations was provided

by NOTUR (Norwegian High Performance Computing Consortium).

References

ACIA 2004. *Impacts of a Warming Climate, Arctic Climate Impact Assessment*. Cambridge University Press, Inc.

Beniston, M., Stephenson, D. B., Christensen, O. B., Ferro, C. A. T., Frei, C., and co-authors. 2007. Future extreme events in European climate: an exploration of regional climate model projections. *Clim. Change* **81**, 71–95, doi:10.1007/s10584–006–9226–z.

Bhattacharyya, G. K. and Johnson, R. A. 1977. *Statistical Concepts and Methods*. John Wiley & Sons, Inc.

Bidlot, J., Hansen, B. and Janssen, P. 1997. Modifications to the ECMWF WAM code. Technical Memorandum 32, ECMWF. ISSN 0332-9879.

Bjørge, D., Haugen, J. E. and Nordeng, T. E. 2000. Future climate in Norway. Research Report 103, Norwegian Meteorological Institute. ISSN 0332-9879.

Blumberg, A. and Mellor, G. 1987. A description of a three-dimensional coastal ocean circulation model. In: *Three-Dimensional Coastal Ocean Models* Volume 4 of Coastal and Estuarine Sciences (ed. N. Heaps), American Geophys. Union, 1–16.

Cairesa, S., Swailb, V. R. and Wang, X. L. 2006. Projection and analysis of extreme wave climate. *J. Climate* **19**, 5581–5605, doi:10.1175/JCLI3918.1.

Christensen, J. H., Machenhauer, B., Jones, R. G., Schär, C., Ruti, P., and co-authors. 1997. Validation of present-day regional climate simulations over Europe: LAM simulations with observed boundary conditions. *Clim. Dyn.* **13**, 489–506.

Christensen, O. B. and Christensen, J. H. 1998. Very high-resolution climate simulation over Scandinavia. Present climate. *J. Climate* **11**, 3204–3229.

Debernard, J. and Køltzow, M. Ø. 2005. Technical documentation of the Oslo Regional Climate Model, version 1.0. Technical Report 8, RegClim General Technical Report. [Available from Norwegian Meteorological Institute, Box 43 Blindern, N-0313 Oslo, Norway].

Debernard, J., Sætra, Ø. and Røed, L. P. 2002. Future wind, wave and storm surge climate in the northern North Atlantic. *Clim. Res.* **23**, 39–49.

Engedahl, H. 1995. Use of the flow relaxation scheme in a three-dimensional baroclinic ocean model with realistic topography. *Tellus* **47A**, 365–382.

Engedahl, H., Lunde, A., Melsom, A. and Shi, X. B. 2001. New schemes for vertical mixing in MI-POM and MICOM. Research Report 118, Norwegian Meteorological Institute. ISSN 0332-9879.

Gjevik, B. and Røed, L. P. 1976. Storm surges along the western coast of norway. *Tellus* **28**, 166–182.

Haugen, J. E. and Iversen, T. 2008. Response in extremes of daily precipitation and wind from a downscaled multi-model ensemble of anthropogenic global climate change scenarios. *Tellus A*, doi:10.1111/j.1600-0870.2008.00315.x.

IPCC 2001. *Climate Change 2001: the Scientific Basis, Technical summary*. http:www.ipcc.ch/pub/wg1TARtechsum.pfd.

Jones, R. G., Murphy, J. M. and Noguer, M. 1995. Simulation of climate-change over Europe using a nested regional-climate model. 1. Assesment of control climate, including sensitivity to location of lateral boundaries. *Q. J. Roy. Met. Soc.* **121B**, 1413–1449.

Jones, R. G., Murphy, J. M., Noguer, M. and Keen, A. B. 1997. Simulation of climate change over Europe using a nested regional-climate model. 2. Comparison of driving and regional model responses to a doubling of carbon dioxide. *Q. J. Roy. Met. Soc.* **123B**, 265–292.

Kauker, F. and Langenberg, H. 2000. Two models for the climate change related development of sea levels in the North Sea—a comparison. *Clim. Res.* **16**, 61–67.

Langenberg, H., Pfizenmayer, A., von Storch, H. and Sündermann, J. 1999. Storm-related sea level variations along the North Sea coast: natural variability and anthropogenic change. *Cont. Shelf. Res.* **19**, 821–842.

Lowe, J. A. and Gregory, J. M. 2005. The effects of climate change on storm surges around the United Kingdom. *Phil. Trans. R. Soc. A* **363**, 1313–1328, doi:10.1098/rsta.2005.1570.

Lowe, J. A., Gregory, J. M. and Flather, R. A. 2001. Changes in the occurence of storm surges around the United Kingdom under a future climate scenario using a dynamic storm surge model driven by the Hadley Centre climate model. *Clim. Dyn.* **18**, 179–188.

Martinsen, E. A., Gjevik, B. and Røed, L. P. 1979. A numerical model for long barotropic waves and storm surges along the western coast of Norway. *J. Phys. Oceanogr.* **9**, 1126–1138.

Pfizenmayer, A. and von Storch, H. 2001. Antropogenic climate change shown by local wave conditions in the North Sea. *Clim. Res.* **19**, 15–23.

Räisänen, J., Hanson, U., Ullerstig, A., Döscher, R., Graham, L. P., and co-authors. 2004. European climate in the late twenty-first century: regional simulations with two driving global models and two forcing scenarios. *Clim. Dyn.* **22**, 13–31, doi:10.1007/s00382–003–0365–x.

STOWASUS-2100 2001. Synthesis of the STOWASUS-2100 project: regional storm, wave and surge scenarios for the 2100 century. Technical Report 01-3, Danish Climate Centre.

WAMDI 1988. The WAM model—a third generation ocean wave prediction model. *J. Phys. Oceanogr.* **18**, 1775–1810.

Wang, X. L. L. and Swail, V. R. 2006. Climate change signal and uncertainty in projections of ocean wave heights. *Clim. Dyn.* **26**, 109–126, doi:10.1007/s00382–005–0080–x.

Wang, X. L. L., Zwiers, F. W. and Swail, V. R. 2004. North Atlantic Ocean wave climate change scenarios for the twenty-first century. *J. Climate* **17**, 2368–2383, doi:10.1175/1520–0442(2004)017.

WASA 1998. Changing waves and storms in the northeast Atlantic? *Bull. Am. Meteorol. Soc.* **79**, 741–760.

WMO 1998. *Guide to wave analysis and forecasting*. WMO-No. 702. Secretariat of the World Meteorological Organization, Geneva, Switzerland.

Woth, K. 2005. Future North Sea storm surge extremes. *Geophys. Res. Lett.* **32**, L22708, doi:10.1029/2005GL023762.

Woth, K., Weisse, R. and von Storch, H. 2006. Climate change and North Sea storm surge extremes: an ensemble study of storm surge extremes expected in a changed climate projected by four different regional climate models. *Ocean Dyn.* **56**, 3–15, doi:10.1007/s10236–005–0024–3.